Available online at www.sciencedirect.com
SCIENCE DIRECT®
Chemical Physics 304 (2004) 183–202
Chemical Physics
www.elsevier.com/locate/chemphys

Time-dependent variational approach to molecules in strong laser fields

Thomas Kreibich [a], Robert van Leeuwen [b], E.K.U. Gross [c,*]

[a] Institut für Theoretische Physik, Am Hubland, D-97074 Würzburg, Germany
[b] Theoretical Chemistry, Materials Science Center, Rijksuniversiteit Groningen, Nijenborgh 4, 9747AG, Groningen, The Netherlands
[c] Institut für Theoretische Physik, Freie Universität Berlin, Arnimallee 14, D-14195 Berlin, Germany

Received 26 January 2004; accepted 20 April 2004
Available online 2 July 2004

Abstract

We study the dynamics of the electronic and nuclear degrees of freedom for molecules in strong laser fields using an ansatz for the wavefunction that explicitly incorporates the electron–nuclear correlation. Equations of motion for this wavefunction are derived on the basis of the stationary action principle. The method is tested on a one-dimensional model of the H_2^+ molecule that can be solved essentially exactly by numerical integration of the time-dependent Schrödinger equation. By comparison with this exact solution we find that the correlated approach improves significantly on a mean-field treatment, especially for laser fields strong enough to cause substantial dissociation. These results are very promising since our method still has a simple orbital structure and can hence be applied to realistic many-electron molecules.

Keywords: Molecules; Intense lasers; Ionization; Dissociation; Action principle

1. Introduction

In recent years, laser technology has dramatically improved such that, nowadays, tabletop systems routinely provide femtosecond laser pulses with intensities in the terawatt regime [1,2]. If atomic and molecular systems are exposed to such extreme radiation fields, a wealth of – sometimes unexpected – fascinating phenomena occurs, opening up novel directions in physics and chemistry.

Owing to their ultra-short duration, femtosecond pulses allow for the direct observation of chemical reactions on the time scale they really occur [3–5]. This has led to tremendous progress in the understanding of chemical (and biological) processes. Moreover an old chemists' dream, namely to control and manipulate chemical reactions by lasers, has become reality [6–8].

By concentrating the radiation energy on the short femtosecond time scale, current laser pulses reach very high intensities. The field strengths at such intensities are comparable to or even larger than typical atomic or molecular binding forces. For instance, the electric field by the atomic nucleus on the first bohr orbit of the hydrogen atom has a field strength of 5.1×10^9 V/m corresponding to an intensity of 3.51×10^{16} W/cm^2 which is an intensity routinely reached by current high-intensity lasers. Irradiation of atoms and molecules by such intense laser pulses gives rise to highly nonlinear effects [9–14] such as multiphoton ionization, above-threshold ionization or dissociation, Coulomb explosion or high-harmonic generation.

As their salient feature, all discussed phenomena are characterized by strong nonlinearities such that perturbative approaches are inevitably bound to fail. Therefore, an adequate description of strong-field multiphoton processes

* Corresponding author. Tel.: +49-30-838-54784; fax: +49-30-838-55258.
E-mail address: hardy@physik.fu-berlin.de (E.K.U. Gross).

0301-0104/$ - see front matter © 2004 Published by Elsevier B.V.
doi:10.1016/j.chemphys.2004.04.016

requires a non-perturbative scheme which treats the external laser field and the internal Coulomb forces of the atom or molecule on equal footing. Whereas, for atomic systems, considerable progress has been made, the situation is far less advanced for molecules since the additional nuclear degrees of freedom tremendously increase the complexity of the problem. Traditionally, one expands the total molecular wavefunction in terms of Born–Oppenheimer (BO) states and solves the resulting time-dependent coupled equations for the nuclei [15]. Typically, the dynamics of the nuclei is treated on the lowest few potential energy surfaces. Including a larger number of electronic states, which is mandatory for high intensity fields, leads to increasingly time-consuming calculations. Moreover, ionization processes are very difficult to treat within this approach. On the other hand, highly excited as well as ionized electrons have been treated within the clamped-nucleus approximation [16–19]. This approach, however, leaves the nuclei fixed and does therefore not allow for the description of dissociation dynamics. Due to their inherent limits, none of these approaches can satisfactorily account for the interplay between electronic excitation and ionization on one hand, and nuclear vibration and dissociation on the other hand. Recent exact numerical solutions for the strong-field dynamics of the H_2^+ molecule [19–24], however, emphasized the need of such a unified treatment. Yet, even for this simplest possible molecule, a full numerical solution is an extremely demanding task and cannot be applied to larger systems. Therefore, finally aiming at ab initio description of the strong-field dynamics of larger molecules, one needs to resort to approximations. In this work we study two different approximations. The first one is a Hartree or mean-field treatment of the electron–nuclear coupling and the second one employs a more sophisticated explicitly correlated ansatz for the electron–nuclear part of the full wavefunction. Our treatment, however, still allows for a description of the system in terms of single particle orbitals. This feature is of great computational advantage for the description of realistic molecules. To test the validity of our ansatz we evaluate our approximations for a one-dimensional model of the H_2^+ molecule for which the exact electron–nuclear wavefunction can be obtained numerically. This approach will lead to valuable insight into the nature of the electron–nuclear correlation for molecules in strong laser fields. It must be stressed, however, that our ultimate goal is to find computationally tractable approximations for realistic many-electron molecules.

2. Basic formalism

2.1. The Hartree approach and an explicitly correlated ansatz for the time-dependent wavefunction

To test our proposed approximations in detail, we employ, in this work, a simplified model of the H_2^+ molecule. In the model, the dimensionality of the problem is reduced by restricting the motion of the nuclei and the electron to the direction of the polarization axis of the laser field [25–27]. In the center-of-mass system, the dynamics of this molecule is governed by the Hamiltonian (employing atomic units)

$$\hat{H}(t) = -\frac{1}{M}\frac{\partial^2}{\partial R^2} + W_{\mathrm{nn}}(R) - \frac{1}{2\mu_{\mathrm{e}}}\frac{\partial^2}{\partial z^2} + W_{\mathrm{en}}(z,R) + \hat{V}_{\mathrm{laser}}(z,t), \tag{1}$$

where R and z denote the internuclear distance and the electronic coordinate as measured from the nuclear center of mass, respectively, and the electronic reduced mass is given by $\mu_{\mathrm{e}} = 2M/(2M+1)$ where M is the proton mass. Employing soft-Coulomb potentials, the particle–particle interactions are given by

$$W_{\mathrm{nn}}(R) = \frac{1}{\sqrt{R^2+\epsilon_{\mathrm{n}}}}, \tag{2}$$

$$W_{\mathrm{en}}(z,R) = -\frac{1}{\sqrt{(z-R/2)^2+\epsilon_{\mathrm{e}}}} - \frac{1}{\sqrt{(z+R/2)^2+\epsilon_{\mathrm{e}}}} \tag{3}$$

with $\epsilon_{\mathrm{e}} = 1$ and $\epsilon_{\mathrm{n}} = 0.03$. The actual values of these parameters are not very important for our benchmark purposes, the value $\epsilon_{\mathrm{e}} = 1$ is a commonly used standard choice and the value $\epsilon_{\mathrm{n}} = 0.03$ is chosen to give a numerically convenient smoothing of the internuclear repulsion. Furthermore, the laser field is represented in the length gauge, $\hat{V}_{\mathrm{laser}}(z,t) = q_{\mathrm{e}} z E(t)$, where $E(t)$ denotes the electric field amplitude and $q_{\mathrm{e}} = (2M+2)/(2M+1)$. In recent years, the reduced-dimensional model was successfully used to analyze the strong-field dynamics of atoms and molecules [28–30]. It has been shown that this model reproduces all the salient strong-field effects such as multiphoton and above-threshold ionization, above-threshold dissociation, or high-harmonic generation. In particular, the model provided valuable insight in the impact of electron–electron correlation effects on strong-field atomic dynamics, such as in the description of non-sequential double ionization [31–35] and non-BO phenomena such as the generation of even harmonics for molecules in intense laser fields [36]. In much the same way, we employ the model to investigate approximations for the electron–nuclear correlation in the context of molecular strong-field dynamics and we use it in

particular to benchmark approximations for the wavefunction. Our reference standard will therefore be the solution of the time-dependent Schrödinger equation

$$(\mathrm{i}\partial_t - \hat{H}(t))\Psi(R,z,t) = 0, \tag{4}$$

where $\hat{H}(t)$ is the Hamiltonian of Eq. (1). Apart from this exact solution we consider two approximate forms of the wavefunction. To determine the equations of motion for these approximate wavefunctions we employ the stationary-action principle [37,38]

$$\delta\mathscr{A}[\Psi] = \delta\int_{t_0}^{t_1} \mathrm{d}t\langle\Psi(t)|\mathrm{i}\partial_t - \hat{H}(t)|\Psi(t)\rangle = 0. \tag{5}$$

Alternatively one may employ the Frenkel variational principle which will lead to the same equations of motion [36]. For any approximate form of the wavefunction Ψ, the stationary-action principle determines the corresponding equations of motion and thus the (approximate) dynamical behavior of the system. To study the importance of electron–nuclear correlation we study two different forms for the wavefunction. The simpler one is the uncorrelated "Hartree" or mean-field form

$$\Psi(R,z,t) = \chi(R,t)\varphi(z,t). \tag{6}$$

This wavefunction is a simple product of a nuclear wavefunction χ and an electronic wavefunction φ. Going beyond the simple Hartree approach we further propose an explicitly correlated ansatz for the full time-dependent wavefunction of the form

$$\Psi(R,z,t) = \chi(R,t)(\phi_1(z-R/2,t) + \phi_2(z+R/2,t)). \tag{7}$$

In Eq. (7), $\chi(R,t)$ denotes the nuclear wavefunction. The electronic degree of freedom, on the other hand, is described by a linear combination of two time-dependent atomic orbitals, each attached to one of the two nuclei. In other words, the correlation between the electron and the nuclei is introduced by referring the electron, in the spirit of a Heitler–London ansatz, to one or the other nucleus. The variationally best orbitals χ, ϕ_1, and ϕ_2 will be determined by equations of motion following from the stationary-action principle (5), leading to an "optimized" approximate time-dependent wavefunction. We will in the following refer to the form in Eq. (7) together with its equations of motion as the correlated time-dependent variational ansatz.

We finally introduce two quantities that play an important role in the calculation of ionization and dissociation probabilities. These are the electronic density $\rho(z,t)$ and the nuclear density $N(R,t)$ defined by

$$\rho(z,t) = \int \mathrm{d}R|\Psi(R,z,t)|^2, \tag{8}$$

$$N(R,t) = \int \mathrm{d}z|\Psi(R,z,t)|^2. \tag{9}$$

The quantity $\rho(z,t)$ gives a probability distribution of finding an electron at the position z as measured from the nuclear center of mass, whereas $N(R,t)$ gives a probability distribution of finding the internuclear distance R. These quantities are easily evaluated for our model wavefunctions. For the simple Hartree or mean-field approach, Eq. (6) leads to

$$N(R,t) = |\chi(R,t)|^2, \tag{10}$$

$$\rho(z,t) = |\varphi(z,t)|^2, \tag{11}$$

whereas, from the correlated variational approach, we obtain from Eq. (7)

$$N(R,t) = |\chi(R,t)|^2\int \mathrm{d}z|\phi_1(z-R/2,t) + \phi_2(z+R/2,t)|^2, \tag{12}$$

$$\rho(z,t) = \int \mathrm{d}R|\chi(R,t)|^2|\phi_1(z-R/2,t) + \phi_2(z+R/2,t)|^2. \tag{13}$$

By integrating these probability distributions over space we will later define the ionization and dissociation probabilities of the molecule in the presence of a laser field.

2.2. The equations of motion

Let us start out by deriving the equations of motion for our approximate wavefunctions. Inserting the Hartree ansatz (6) into the stationary action principle (5) we find the equations of motion [39]

$$\mathrm{i}\partial_t\chi(R,t) = \left(-\frac{1}{M}\frac{\mathrm{d}^2}{\mathrm{d}R^2} + W_{\mathrm{nn}}(R) + \int \mathrm{d}z|\varphi(z,t)|^2 W_{\mathrm{en}}(z,R)\right)\chi(R,t), \tag{14}$$

$$\mathrm{i}\partial_t\varphi(z,t) = \left(-\frac{1}{2\mu_{\mathrm{e}}}\frac{\mathrm{d}^2}{\mathrm{d}z^2} + q_{\mathrm{e}}zE(t) + \int \mathrm{d}R|\chi(R,t)|^2 W_{\mathrm{en}}(z,R)\right)\varphi(z,t). \tag{15}$$

In this mean field approximation the potentials of the nuclear and electronic wavefunctions are thus found by averaging the electronic and nuclear densities over the electron–nuclear interaction W_{en}. Let us now discuss the more sophisticated correlated ansatz. By employing the time-dependent variational principle (5), we again determine the variationally best wavefunction of the form (7). To this end, the trial wavefunction (7) is inserted into the action functional (5). This yields

$$\begin{aligned}\mathscr{A}[\chi,\phi_1,\phi_2] = \int \mathrm{d}t \int \mathrm{d}R\,\mathrm{d}z \Big\{ &|\varphi_R(z,t)|^2 \chi^\star(R,t)\left(\mathrm{i}\partial_t - \hat{T}_{\mathrm{n}} - \hat{W}_{\mathrm{nn}}\right)\chi(R,t) \\ &+ \frac{1}{\mu_{\mathrm{n}}}\left(\chi^\star(R,t)\frac{\mathrm{d}}{\mathrm{d}R}\chi(R,t)\right)\left(\varphi_R^\star(z,t)\frac{\mathrm{d}}{\mathrm{d}R}\varphi_R(z,t)\right) + |\chi(R,t)|^2\varphi_R^\star(z,t)\left(\mathrm{i}\partial_t - \hat{T}_{\mathrm{n}} - \hat{H}_{\mathrm{e}}\right)\varphi_R(z,t)\Big\},\end{aligned} \tag{16}$$

where $\varphi_R(z,t) := \phi_1(z - R/2,t) + \phi_2(z + R/2,t)$ and $\hat{H}_{\mathrm{e}} := \hat{T}_{\mathrm{e}} + \hat{W}_{\mathrm{en}} + \hat{V}_{\mathrm{laser}}(t)$. Note that, due to the dependence of $\varphi_R(z,t)$ on special combinations of the nuclear and electronic coordinate, the action of the nuclear momentum operator on $\varphi_R(z,t)$ is easily expressed in terms of the electronic momentum operator.

The equations of motion which determine the optimized orbitals χ, ϕ_1, and ϕ_2 are obtained by requiring the action functional (16) to be stationary with respect to variations of all orbitals, i.e.,

$$\frac{\delta\mathscr{A}[\chi,\phi_1,\phi_2]}{\delta\chi^\star(R,t)} = 0, \tag{17}$$

$$\frac{\delta\mathscr{A}[\chi,\phi_1,\phi_2]}{\delta\phi_1^\star(z,t)} = 0, \tag{18}$$

$$\frac{\delta\mathscr{A}[\chi,\phi_1,\phi_2]}{\delta\phi_2^\star(z,t)} = 0. \tag{19}$$

At this point it is important to note that the ansatz (7) for the full wavefunction Ψ is invariant under the transformation

$$\chi \to c(t)\cdot\chi, \quad \phi_{1/2} \to \frac{1}{c(t)}\cdot\phi_{1/2}, \tag{20}$$

where $c(t)$ is a purely time-dependent but otherwise arbitrary complex function. As a consequence of this invariance property (20) of the wavefunction, Eqs. (17)–(19) are not sufficient to *uniquely* determine the time evolution of the orbitals χ, ϕ_1, and ϕ_2. To fix the freedom expressed in Eq. (20), we need an additional constraint. As a convenient choice, we may require

$$\langle\chi|\partial_t\chi\rangle = 0, \tag{21}$$

which fixes the norm and the phase of $\chi(R,t)$ and hence the purely time-dependent function $c(t)$ (a similar technique is used in the so-called time-dependent extended Hartree–Fock method [33,34]). Together with the constraint (21), the equations of motion (17)–(19) now have a unique solution. We should note that a similar invariance applies to the Hartree approximation (6), but since within this approximation the equations of motion, Eqs. (14) and (15), for χ and φ are hermitian and hence conserve the norm of these orbitals, the function $c(t)$ is completely determined by the choice of the initial wavefunctions. By performing the variations in Eqs. (17)–(19), we obtain

$$\begin{aligned}\frac{\delta\mathscr{A}}{\delta\chi^\star(R,t)} = \int \mathrm{d}z \Big\{ &|\varphi_R(z,t)|^2\left(\mathrm{i}\partial_t - \hat{T}_{\mathrm{n}} - W_{\mathrm{nn}}(R)\right)\chi(R,t) + \frac{1}{\mu_{\mathrm{n}}}\left(\varphi_R^\star(z,t)\frac{\mathrm{d}}{\mathrm{d}R}\varphi_R(z,t)\right)\frac{\mathrm{d}}{\mathrm{d}R}\chi(R,t) \\ &+ \left(\varphi_R^\star(z,t)\left(\mathrm{i}\partial_t - \hat{T}_{\mathrm{n}} - \hat{H}_{\mathrm{e}}\right)\varphi_R(z,t)\right)\chi(R,t)\Big\},\end{aligned} \tag{22}$$

$$\begin{aligned}\frac{\delta\mathscr{A}}{\delta\phi_1^\star(z,t)} = \int \mathrm{d}R \Big\{ &\left(\chi^\star(R,t)\left(\mathrm{i}\partial_t - \hat{T}_{\mathrm{n}} - \hat{W}_{\mathrm{nn}}\right)\chi(R,t)\right)(\phi_1(z,t) + \phi_2(z+R,t)) - \frac{1}{2\mu_{\mathrm{n}}}\left(\chi^\star(R,t)\frac{\mathrm{d}}{\mathrm{d}R}\chi(R,t)\right)\frac{\mathrm{d}}{\mathrm{d}z}(\phi_1(z,t) \\ &- \phi_2(z+R,t)) + |\chi(R,t)|^2\left(\mathrm{i}\partial_t + \frac{1}{2\tilde{\mu}_{\mathrm{e}}}\frac{\mathrm{d}^2}{\mathrm{d}z^2} - W_{\mathrm{en}}(z+R/2,R) - V_{\mathrm{laser,e}}(z+R/2,t)\right) \\ &\times(\phi_1(z,t) + \phi_2(z+R,t))\Big\},\end{aligned} \tag{23}$$

$$\frac{\delta\mathcal{A}}{\delta\phi_2^\star(z,t)} = \int \mathrm{d}R\Big\{\Big(\chi^\star(R,t)\Big(\mathrm{i}\partial_t - \hat{T}_\mathrm{n} - \hat{W}_\mathrm{nn}\Big)\chi(R,t)\Big)(\phi_1(z-R,t)+\phi_2(z,t)) - \frac{1}{2\mu_\mathrm{n}}\left(\chi^\star(R,t)\frac{\mathrm{d}}{\mathrm{d}R}\chi(R,t)\right)$$
$$\times\frac{\mathrm{d}}{\mathrm{d}z}(\phi_1(z-R,t)-\phi_2(z,t)) + |\chi(R,t)|^2\left(\mathrm{i}\partial_t + \frac{1}{2\tilde{\mu}_\mathrm{e}}\frac{\mathrm{d}^2}{\mathrm{d}z^2} - W_\mathrm{en}(z-R/2,R) - V_\mathrm{laser,e}(z-R/2,t)\right)$$
$$\times(\phi_1(z-R,t)+\phi_2(z,t))\Big\}, \tag{24}$$

where the action of the nuclear kinetic-energy operator on the atomic orbitals is reflected in the change of the electronic reduced mass μ_e to $\tilde{\mu}_\mathrm{e} = 4\mu_\mathrm{n}\mu_\mathrm{e}/(4\mu_\mathrm{n}+\mu_\mathrm{e})$. For the ease of notation, we introduce the following abbreviations:

$$\langle\hat{\mathcal{O}}\rangle_\mathrm{e} \equiv \langle\hat{\mathcal{O}}\rangle_\mathrm{e}(R,t) := \frac{\langle\varphi_R|\hat{\mathcal{O}}|\varphi_R\rangle_\mathrm{e}}{\langle\varphi_R|\varphi_R\rangle_\mathrm{e}}, \tag{25}$$

$$\langle\hat{\mathcal{O}}\rangle_\mathrm{n} \equiv \langle\hat{\mathcal{O}}\rangle_\mathrm{n}(z,t) := \frac{\langle\chi|\hat{\mathcal{O}}|\chi\rangle_\mathrm{n}}{\langle\chi|\chi\rangle_\mathrm{n}}, \tag{26}$$

where $\hat{\mathcal{O}}$ denotes an arbitrary operator in the relevant Hilbert space and the subscripts "e" or "n" indicate the integration over the electronic or nuclear coordinate, respectively. Of course, the dependence of (26) on z vanishes if the operator $\hat{\mathcal{O}}$ only depends on the nuclear coordinate.

Employing Eq. (22) in the variation (17) subject to the condition (21) we obtain the *nuclear equation of motion*:

$$\mathrm{i}\partial_t\chi(R,t) = \Big(\hat{h}_\mathrm{n}(R,t) - \Lambda(t)\Big)\chi(R,t) \tag{27}$$

with the effective nuclear Hamiltonian

$$\hat{h}_\mathrm{n}(R,t) := -\frac{1}{2\mu_\mathrm{n}}\frac{\mathrm{d}^2}{\mathrm{d}R^2} - \frac{1}{\mu_\mathrm{n}}\left\langle\frac{\mathrm{d}}{\mathrm{d}R}\right\rangle_\mathrm{e}(R,t)\frac{\mathrm{d}}{\mathrm{d}R} + \langle\hat{H}-\mathrm{i}\partial_t\rangle_\mathrm{e}(R,t) \tag{28}$$

and

$$\Lambda(t) = \langle\hat{h}_\mathrm{n}\rangle_\mathrm{n}(t). \tag{29}$$

The purely time-dependent, in general, complex function $\Lambda(t)$ is introduced to satisfy the constraint (21). From the nuclear equation of motion (27), it is easily seen that the change in χ is always orthogonal to χ, as required by (21).

Analogously, by inserting Eqs. (23) and (24) in Eqs. (18) and (19), we obtain the *equations of motion for the electronic atomic orbitals*:

$$\mathrm{i}\partial_t\phi_1(z,t) = \hat{h}_{\mathrm{e},1}\phi_1(z,t) + \mathcal{Q}_1(z,t), \tag{30}$$

$$\mathrm{i}\partial_t\phi_2(z,t) = \hat{h}_{\mathrm{e},2}\phi_2(z,t) + \mathcal{Q}_2(z,t), \tag{31}$$

where

$$\hat{h}_{\mathrm{e},1} := -\frac{1}{2\tilde{\mu}_\mathrm{e}}\frac{\mathrm{d}^2}{\mathrm{d}z^2} + \frac{1}{2\mu_\mathrm{n}}\left\langle\frac{\mathrm{d}}{\mathrm{d}R}\right\rangle_\mathrm{n}(t)\frac{\mathrm{d}}{\mathrm{d}z} + \left\langle\hat{H}\left(z+\frac{R}{2},R\right) - \hat{T}_\mathrm{e} - \mathrm{i}\partial_t\right\rangle_\mathrm{n}(z,t), \tag{32}$$

$$\hat{h}_{\mathrm{e},2} := -\frac{1}{2\tilde{\mu}_\mathrm{e}}\frac{\mathrm{d}^2}{\mathrm{d}z^2} - \frac{1}{2\mu_\mathrm{n}}\left\langle\frac{\mathrm{d}}{\mathrm{d}R}\right\rangle_\mathrm{n}(t)\frac{\mathrm{d}}{\mathrm{d}z} + \left\langle\hat{H}\left(z-\frac{R}{2},R\right) - \hat{T}_\mathrm{e} - \mathrm{i}\partial_t\right\rangle_\mathrm{n}(z,t) \tag{33}$$

represent the effective electronic Hamiltonians and

$$\mathcal{Q}_1(z,t) := \langle(\hat{H}(z+R/2,R) - \mathrm{i}\partial_t)\phi_2(z+R,t)\rangle_\mathrm{n}(z,t), \tag{34}$$

$$\mathcal{Q}_2(z,t) := \langle(\hat{H}(z-R/2,R) - \mathrm{i}\partial_t)\phi_1(z-R,t)\rangle_\mathrm{n}(z,t) \tag{35}$$

denote the inhomogeneity terms in Eqs. (30) and (31).

Eqs. (27), (30) and (31) constitute the time-dependent variational scheme which governs the (approximate) time evolution of the H_2^+ molecule considered here. It appears well suited for a theoretical description of the strong-field dynamics of molecular systems since, first of all, it provides a non-perturbative approach which allows one to treat the strong external fields and the intramolecular forces on the same footing. Furthermore, the method properly accounts for the quantum nature of both the electronic and the nuclear degrees of freedom. In this respect, the proposed

variational approach goes beyond mixed classical-quantum mechanical methods where the nuclear dynamics is treated only classically. On the other hand, in contrast to methods employing wavepacket propagations on few BO potential energy surfaces, the influence of the strong laser field on the time evolution of the electrons is consistently incorporated, too. Still, although an explicitly correlated ansatz for the total wavefunction is used, it is important to notice that the time evolution of the system is governed by (a set of coupled) single-particle equations. Therefore, the numerical effort to solve the above equations stays manageable.

Considering the above equations of motion individually, we observe the following features: The electronic dynamics is determined by a coupled set of time-dependent Schrödinger equations with additional inhomogeneity terms. This is a consequence of the fact that the time evolution of the system is determined from atomic rather than molecular orbitals. Correspondingly, the inhomogeneities $\mathscr{Q}_{1/2}$ have a clear physical interpretation: They act as source or sink terms and are thus responsible for the (laser-induced) transfer of electronic charge between the two nuclei. Considering the effective electronic potentials, the contribution arising from the electron–nuclear interaction is given by

$$\langle W_{\mathrm{en}}(z \pm R/2, R)\rangle_{\mathrm{n}}(z,t) = -\frac{1}{\sqrt{R^2+\epsilon_{\mathrm{e}}}} - \frac{1}{\langle\chi|\chi\rangle}\int \mathrm{d}R \frac{|\chi(R,t)|^2}{\sqrt{(z\pm R)^2+\epsilon_{\mathrm{e}}}}. \tag{36}$$

Accordingly, the electron feels the bare Coulomb force of its reference nucleus and a Hartree-type potential from the second nucleus. Due to the dependence of (36) on the time-dependent orbital $\chi(R,t)$, the electronic potential immediately reacts on changes of the internuclear separation. Therefore, we can expect the variational scheme to properly describe typical strong-field effects such as charge resonance enhanced ionization (CREI) [40,41] followed by Coulomb explosion or the dynamical Stark shift. To elucidate this statement, consider a dissociating molecule: In this case, part of the nuclear density is represented by wavepackets which travel to larger internuclear separations. This enlargement of the internuclear separation is subsequently reflected in changes of the electronic potentials, lowering the binding forces on the electron. As a consequence, enhanced ionization occurs for some critical internuclear distance. The ionization process acts back on the nuclei by changing the nuclear effective potential. In the BO language, this amounts to non-adiabatic transitions between different BO potential energy surfaces. Specifically, for the H_2^+ molecule, the nuclear potential only consists of the nuclear–nuclear interaction once the electron is ionized, such that the molecule explodes due to Coulomb repulsion. Therefore, the CREI followed by Coulomb explosion should be naturally included within the time-dependent variational approach.

Turning towards the nuclear equation of motion (27), we find that it resembles the one used in traditional wavepacket propagation schemes. However, due to the time-dependence of the effective potential, given by the expectation value of $\hat{H} - \mathrm{i}\partial_t$ with respect to $\varphi_R(z,t)$, the dynamics is not restricted to a fixed potential energy surface, but non-adiabatic processes can be described even by employing only one (time-dependent) nuclear potential. Furthermore, due to the Heitler–London-type form of φ_R, the nuclear potential has the correct asymptotic ($R \to \infty$) limit. Additionally, Eq. (27) contains a term proportional to the nuclear momentum operator which acts as a vector potential.

3. Normalization, symmetry and ground state

We now turn to some questions that play a role when we want to propagate the equations of motion, such as the conservation of the norm of the wavefunction. It is important to realize that the property of norm conservation is preserved for any approximate wavefunction, provided it obeys the variational equation of motion. This is most easily seen by considering an approximate wavefunction $\tilde{\Psi}$ which makes the action stationary. Then, a variation $\tilde{\Psi} \to \mathrm{e}^{\mathrm{i}\alpha(t)}\tilde{\Psi}$ with $\alpha(t_0) = \alpha(t_1) = 0$ does not change the action

$$0 = \delta\mathscr{A} = \mathscr{A}[\mathrm{e}^{\mathrm{i}\alpha(t)}\tilde{\Psi}] - \mathscr{A}[\tilde{\Psi}] = -\int_{t_0}^{t_1} \mathrm{d}t\langle\tilde{\Psi}|\tilde{\Psi}\rangle\partial_t\alpha(t) = \int_{t_0}^{t_1} \mathrm{d}t\alpha(t)\partial_t\langle\tilde{\Psi}|\tilde{\Psi}\rangle. \tag{37}$$

Since $\alpha(t)$ is arbitrary for $t_0 < t < t_1$, we find

$$\partial_t\langle\tilde{\Psi}|\tilde{\Psi}\rangle = 0 \tag{38}$$

for an arbitrary approximate wavefunction $\tilde{\Psi}$ which obeys the equations of motion derived from the stationary-action principle – although no normalization constraint or Lagrange multiplier had been used. For this reason the norms of our approximate wavefunctions (Eqs. (6) and (7)) are conserved since the equations of motion are derived from the action principle. For the Hartree ansatz this is also easily seen from the corresponding equations of motion since they are hermitian. Norm conservation is less obvious for the correlated ansatz but can, of course, also be directly verified from the equations of motion. To that end, we first observe that

$$\int \mathrm{d}z \left(\phi_1^\star(z,t) \frac{\delta \mathscr{A}[\chi,\phi_1,\phi_2]}{\delta \phi_1^\star(z,t)} + \phi_2^\star(z,t) \frac{\delta \mathscr{A}[\chi,\phi_1,\phi_2]}{\delta \phi_2^\star(z,t)} \right) = 0, \tag{39}$$

where we explicitly used the electronic equations of motion (18) and (19). The left-hand side of Eq. (39) is the Lagrangian corresponding to the approximate wavefunction (7), $\mathscr{L} := \langle \Psi | \mathrm{i}\partial_t - \hat{H} | \Psi \rangle$. Therefore, $\mathscr{L}$ vanishes identically

$$\mathscr{L} = \langle \Psi | \mathrm{i}\partial_t - \hat{H} | \Psi \rangle = 0. \tag{40}$$

We note in passing that, as a consequence of Eq. (40), the action vanishes at the solution point, too. This is true for the exact solution of the time-dependent Schrödinger equation as well as for any approximate wavefunction which makes the action stationary. Hence, the value of the action does – in contrast to, e.g., the energy in the static case – not provide any valuable quantity to assess the quality of the approximation employed.

Furthermore, Eq. (40) implies that

$$\langle \Psi | \mathrm{i}\partial_t - \hat{H} | \Psi \rangle - \langle \Psi | \mathrm{i}\partial_t - \hat{H} | \Psi \rangle^\star = \mathrm{i}\partial_t \langle \Psi | \Psi \rangle = 0, \tag{41}$$

since $\hat{H}$ is an hermitian operator. Therefore, the conservation of the norm of the full time-dependent wavefunction Ψ is automatically guaranteed, provided the orbitals χ, ϕ_1, and ϕ_2 obey the equations of motion (27), (30) and (31).

The norm of the single-particle orbitals is, on the other hand, not necessarily conserved. This is due to the fact that the equations of motion are, in general, not hermitian. In fact, considering the norm of the electronic atomic orbital, one obtains

$$\partial_t \ln \langle \phi_{1/2} | \phi_{1/2} \rangle = -2\mathrm{i}\,\mathrm{Im} \frac{\langle \phi_{1/2} | \mathscr{Q}_{1/2} \rangle}{\langle \phi_{1/2} | \phi_{1/2} \rangle}, \tag{42}$$

which confirms our previous observation that the inhomogeneity $\mathscr{Q}_{1/2}$ acts as a source or sink term. Thus, they may induce the flow of electronic charge from one orbital to the other, reflecting the transfer of electronic charge between the two nuclei, which leads to variations of the single-particle norms. For the nuclear single-particle orbitals $\chi(R,t)$, the corresponding orbital norm is again conserved

$$\partial_t \langle \chi | \chi \rangle = 0, \tag{43}$$

which immediately follows from the constraint (21). We note that other choices to fix the invariance (20) could change Eqs. (42) and (43), of course, without affecting the norm of the full wavefunction.

We now turn towards a brief discussion of some symmetry properties of the proposed ansatz. Let us first discuss parity transformations. In the ansatz (7), we did not impose any specific behavior of the wavefunction under parity transformations. However, once the external fields vanish, parity is a good quantum number and it is advantageous to choose the wavefunction as an eigenfunction of the parity operator. Consequently, the total ground-state wavefunction then behaves with respect to parity transformations according to

$$\Psi_0(R,-z) = \Psi_0(R,z). \tag{44}$$

A similar symmetry must be obeyed by our approximate wavefuntions. A quick investigation of the Hartree expression shows that it obeys this symmetry. We then turn to the correlated wavefunction. In order to find the equations which determine the ground state of the system, we consider the following time-dependence of the orbitals: $\phi_{1/2}(z,t) \to \mathrm{e}^{-\mathrm{i}\epsilon_\mathrm{e} t} \phi_{1/2}(z)$ and $\chi(R,t) \to \chi(R)$. The nuclear orbital does not carry any time-dependent exponential, since the phase of χ is already fixed by the constraint (21). We therefore obtain using Eqs. (27) and (28) the nuclear eigenvalue equation

$$\left(-\frac{1}{2\mu_\mathrm{n}} \frac{\mathrm{d}^2}{\mathrm{d}R^2} - \frac{1}{\mu_\mathrm{n}} \left\langle \frac{\mathrm{d}}{\mathrm{d}R} \right\rangle_\mathrm{e}(R) \frac{\mathrm{d}}{\mathrm{d}R} + \langle \hat{H} \rangle_\mathrm{e}(R) - \epsilon_\mathrm{n} \right) \chi(R) = 0, \tag{45}$$

where $\epsilon_\mathrm{n} = \epsilon_\mathrm{e} + \Lambda$. It is further readily verified that $\epsilon_\mathrm{n} = \langle \hat{H} \rangle$ i.e., the lowest eigenvalue of Eq. (45) is equal to the ground-state energy of the system, defined as the expectation value of our variation ansatz with respect to the full ground-state Hamiltonian of Eq. (1) in the absence of the laser field. For the ground-state electronic atomic orbitals, we further find

$$\phi_1(z) = \phi(z), \quad \phi_2(z) = \phi(-z), \tag{46}$$

where $\phi(z)$ obeys

$$\left(-\frac{1}{2\tilde{\mu}_\mathrm{e}} \frac{\mathrm{d}^2}{\mathrm{d}z^2} + \frac{1}{2\mu_\mathrm{n}} \left\langle \frac{\mathrm{d}}{\mathrm{d}R} \right\rangle_\mathrm{n} \frac{\mathrm{d}}{\mathrm{d}z} + \langle \hat{H}(z+R/2,R) - \hat{T}_\mathrm{e} \rangle_\mathrm{n}(z) - \epsilon_\mathrm{e} \right) \phi(z) = \langle (\hat{H}(z+R/2,R) - \epsilon_\mathrm{e}) \phi(-z-R) \rangle_\mathrm{n}. \tag{47}$$

By virtue of Eq. (47), the electron is described by a hydrogen-type Schrödinger equation with additional terms arising from the influence of the second nucleus. Hence, the orbital $\phi(z)$ corresponds to a polarized hydrogenic orbital. The atomic orbital itself does not possess a definite symmetry with respect to parity transformations. Nevertheless, the total wavefunction is an even (gerade) state, since, as a consequence of Eq. (46), $\phi_1(z) = \phi_2(-z)$. Therefore, the full ground-state wavefunction has the correct symmetry property.

4. Numerical considerations

In this section, we shall describe the main aspects of our numerical implementation. For the solution of the exact Schrödinger equation (4) and the Hartree mean field equations (14) and (15) the equations are expressed numerically on a finite difference grid and propagated using the split-operator method. Since this is a standard procedure we will not go into the details. The equations of motion for the correlated variational ansatz have a rather different nature. In particular, they are non-hermitian and contain source and sink terms. The solution of these equations requires non-standard methods. The main purpose of this section is to outline the main features of our procedure.

Considering the electronic problem, we have to deal with the set of coupled non-hermitian integro-differential equations (30) and (31) which, in particular, contain complex potentials and inhomogeneity terms. In order to solve these equations the electronic atomic orbitals are expanded according to

$$\phi_1(z,t) = \sum_n a_n(t)\zeta_n(z,t), \tag{48}$$

$$\phi_2(z,t) = \sum_n b_n(t)\zeta_n(z,t). \tag{49}$$

We note that both atomic orbitals are expanded in the same set of basis functions. Naturally, if heteronuclear molecules are to be considered, different basis functions corresponding to the different nuclei could be employed.

Inserting Eqs. (48) and (49) in the electronic equations of motion (30) and (31), one obtains the following matrix equation:

$$\mathrm{i}\sum_m \mathscr{S}_{nm}(t)\begin{pmatrix}\dot{a}_m(t)\\ \dot{b}_m(t)\end{pmatrix} = -\sum_m \mathscr{A}_{nm}(t)\begin{pmatrix}a_m(t)\\ b_m(t)\end{pmatrix}. \tag{50}$$

Here

$$\mathscr{S}_{nm}(t) := \int \mathrm{d}R|\chi(R,t)|^2\begin{pmatrix}\langle n-|m-\rangle_\mathrm{e} & \langle n-|m+\rangle_\mathrm{e}\\ \langle n+|m-\rangle_\mathrm{e} & \langle n+|m+\rangle_\mathrm{e}\end{pmatrix} \tag{51}$$

and

$$\begin{aligned}\mathscr{A}_{nm}(t) := \int \mathrm{d}R\Bigg\{ &\left(\chi^\star(R,t)\left(\hat{T}_\mathrm{n} + \hat{W}_\mathrm{nn} - \mathrm{i}\partial_t\right)\chi(R,t)\right)\begin{pmatrix}\langle n-|m-\rangle_\mathrm{e} & \langle n-|m+\rangle_\mathrm{e}\\ \langle n+|m-\rangle_\mathrm{e} & \langle n+|m+\rangle_\mathrm{e}\end{pmatrix}\\ &-\frac{1}{\mu_\mathrm{n}}\left(\chi^\star(R,t)\frac{\mathrm{d}}{\mathrm{d}R}\chi(R,t)\right)\begin{pmatrix}\langle n-|\frac{\mathrm{d}}{\mathrm{d}R}|m-\rangle_\mathrm{e} & \langle n-|\frac{\mathrm{d}}{\mathrm{d}R}|m+\rangle_\mathrm{e}\\ \langle n+|\frac{\mathrm{d}}{\mathrm{d}R}|m-\rangle_\mathrm{e} & \langle n+|\frac{\mathrm{d}}{\mathrm{d}R}|m+\rangle_\mathrm{e}\end{pmatrix}\\ &+|\chi(R,t)|^2\begin{pmatrix}\langle n-|\hat{T}_\mathrm{n}+\hat{H}_\mathrm{e}-\mathrm{i}\partial_t|m-\rangle_\mathrm{e} & \langle n-|\hat{T}_\mathrm{n}+\hat{H}_\mathrm{e}-\mathrm{i}\partial_t|m+\rangle_\mathrm{e}\\ \langle n+|\hat{T}_\mathrm{n}+\hat{H}_\mathrm{e}-\mathrm{i}\partial_t|m-\rangle_\mathrm{e} & \langle n+|\hat{T}_\mathrm{n}+\hat{H}_\mathrm{e}-\mathrm{i}\partial_t|m+\rangle_\mathrm{e}\end{pmatrix}\Bigg\}\end{aligned} \tag{52}$$

denote the overlap and action matrix, respectively, and the corresponding matrix elements $\langle n\pm|\hat{\mathscr{O}}|m\pm\rangle_\mathrm{e}$ are defined by

$$\langle n\pm|\hat{\mathscr{O}}|m\pm\rangle_\mathrm{e} \equiv \langle n\pm|\hat{\mathscr{O}}|m\pm\rangle_\mathrm{e}(R,t) := \int \mathrm{d}z\zeta_\mathrm{n}^\star\left(z\pm\frac{R}{2},t\right)\mathscr{O}(R,z)\zeta_m\left(z\pm\frac{R}{2},t\right). \tag{53}$$

By virtue of Eq. (50), the time evolution of the electronic degree of freedom is now governed by a system of coupled first-order differential equations. For given matrices $\mathscr{S}$ and $\mathscr{A}$, the time derivatives of the coefficients, $\dot{a}_m(t)$ and $\dot{b}_m(t)$, are obtained by solving the set of linear equation (50). Subsequently, the coefficients are evolved in time by employing the Adams–Bashford–Mouton predictor–corrector scheme of fourth order [45]. The numerical effort is essentially determined by the properties of the overlap matrix $\mathscr{S}$, which depend on the actual choice of the basis functions. The preferred choice of basis functions depends on the physical situation. To study the ground-state solution of Eq. (47) it is convenient to expand in localized orbitals. For this situation we choose the basis functions of the form

$$\zeta_\mathrm{n}(z) := z^{\nu_j}\phi_j^\mathrm{H}(z), \tag{54}$$

where ϕ_j^{H} is a hydrogenic orbital of the soft-Coulomb Schrödinger equation

$$\left(-\frac{1}{2}\frac{\mathrm{d}^2}{\mathrm{d}z^2}-\frac{1}{\sqrt{z^2+\epsilon_{\mathrm{e}}}}-\epsilon_j\right)\phi_j^{\mathrm{H}}(z)=0 \tag{55}$$

and $n=(j,v_j)$ is a cumulative index. For the description of ionization processes in strong laser fields, localized basis functions are not a particularly well-suited choice. Instead, for our time-dependent work we employ delocalized momentum space wavefunctions:

$$\zeta_k(z)=\frac{1}{2\pi}\mathrm{e}^{\mathrm{i}kz}. \tag{56}$$

(The discrete index n has been changed to the continuous variable k and the expansion coefficients a_{n} and b_{n} are replaced by $\tilde{\phi}_1(k)$ and $\tilde{\phi}_2(k)$, respectively.) Besides its evident flexibility, the momentum space basis (56) leads to a reduction of the numerical effort, since the overlap matrix $\mathscr{S}(t)$ acquires a particularly simple structure. By employing

$$\langle k\sigma|k'\sigma'\rangle_{\mathrm{e}}=\frac{1}{2\pi}\mathrm{e}^{\mathrm{i}k(\sigma-\sigma')R/2}\delta(k-k'),\quad \sigma,\sigma'=+1,-1, \tag{57}$$

we immediately find that $\mathscr{S}(t)$ is block diagonal in momentum space. Accordingly, the left-hand side of the electronic equation of motion (50) decouples in momentum space, and only a two-dimensional sub-system of linear equations has to be solved in each time step

$$\mathrm{i}\begin{pmatrix}\langle\chi|\chi\rangle_{\mathrm{n}} & \langle\chi|\mathrm{e}^{\mathrm{i}kR}|\chi\rangle_{\mathrm{n}}\\ \langle\chi|\mathrm{e}^{-\mathrm{i}kR}|\chi\rangle_{\mathrm{n}} & \langle\chi|\chi\rangle_{\mathrm{n}}\end{pmatrix}\begin{pmatrix}\dot{\tilde{\phi}}_1(k,t)\\ \dot{\tilde{\phi}}_2(k,t)\end{pmatrix}=\begin{pmatrix}f_1(k,t)\\ f_2(k,t)\end{pmatrix} \tag{58}$$

with

$$\begin{pmatrix}f_1(k,t)\\ f_2(k,t)\end{pmatrix}:=-\int \mathrm{d}k'\mathscr{A}(k,k',t)\begin{pmatrix}\tilde{\phi}_1(k',t)\\ \phi_2(k',t)\end{pmatrix}. \tag{59}$$

For $k\neq 0$, Eq. (58) is readily solved, yielding

$$\mathrm{i}\dot{\tilde{\phi}}_1(k,t)=\frac{1}{\det(\mathscr{S})}\left(\langle\chi|\chi\rangle_{\mathrm{n}}f_1(k,t)-\langle\chi|\mathrm{e}^{\mathrm{i}kR}|\chi\rangle_{\mathrm{n}}f_2(k,t)\right), \tag{60}$$

$$\mathrm{i}\dot{\tilde{\phi}}_2(k,t)=\frac{1}{\det(\mathscr{S})}\left(-\langle\chi|\mathrm{e}^{-\mathrm{i}kR}|\chi\rangle_{\mathrm{n}}f_1(k,t)+\langle\chi|\chi\rangle_{\mathrm{n}}f_2(k,t)\right) \tag{61}$$

with

$$\det(\mathscr{S})=|\langle\chi|\chi\rangle_{\mathrm{n}}|^2-|\langle\chi|\mathrm{e}^{\mathrm{i}kR}|\chi\rangle_{\mathrm{n}}|^2. \tag{62}$$

For $k=0$, Eq. (58) is not invertible. Physically speaking, this is due to the fact that, for zero momentum, one cannot distinguish between plane waves moving in the different directions. However, one can show that all relevant quantities only depend on the combination $\tilde{\phi}_1(0)+\tilde{\phi}_2(0)$, which can be determined from

$$\mathrm{i}\left(\dot{\tilde{\phi}}_1(0,t)+\dot{\tilde{\phi}}_2(0,t)\right)=\frac{1}{\langle\chi|\chi\rangle_{\mathrm{n}}}f_1(0,t)=\frac{1}{\langle\chi|\chi\rangle_{\mathrm{n}}}f_2(0,t). \tag{63}$$

Eqs. (60), (61) and (63) now govern the time evolution of the Fourier components of the atomic orbitals ϕ_1 and ϕ_2. All quantities depending on the electronic orbitals, i.e., effective potentials like the terms on the right-hand side of Eq. (58) or the effective nuclear Hamiltonian (28) as well as various observables can be efficiently evaluated by means of fast Fourier transform (FFT) methods. In particular, for the calculation of matrix elements involving the interaction potential $W_{\mathrm{en}}(z,R)$, the atomic orbitals are first transformed into configuration space, then multiplied with the interaction potential, and subsequently transformed back to Fourier space. Thus, we circumvent the problem of calculating the Fourier transform of the (soft-) Coulomb potentials, which diverges at $k=0$. All other terms are directly expressed in terms of the momentum space basis functions.

The nuclear equation of motion, Eq. (27), on the other hand, is represented on a finite-difference grid and integrated by employing the implicit Crank–Nicholson algorithm. In order to account for the dependence of the effective nuclear Hamiltonian $\hat{h}_{\mathrm{n}}(R,t)$ on the time-derivatives of the electronic orbitals at time t, a predictor–corrector scheme is additionally employed.

5. Results

5.1. Ground state

In order to solve the ground-state Eqs. (45) and (47), we proceed as in the previous section. Accordingly, the nuclear equation is represented on a finite-difference grid, while the electronic orbitals are expanded in a set of basis functions. Thus, Eq. (47) is rewritten as a (generalized) eigenvalue problem. The resulting equations are then iterated until self-consistency is achieved. For that purpose, the basis set was most conveniently chosen as in Eq. (54). We find excellent convergence for five basis functions ($j = 0,\ v_0 = 0,\ldots,4$). In Fig. 1, we have plotted the effective nuclear potential $V_n(R) = \langle \hat{H} \rangle_e(R)$ obtained from a self-consistent solution of the variational equations. For comparison, we have added the nuclear potentials resulting from the BO, and the Hartree approximation. Evidently, the nuclear potential of the variational scheme is almost identical to the exact one in the region of non-vanishing nuclear density, i.e., for $1 \lesssim R \lesssim 4.5$ a.u. Correspondingly, the ground-state energy $E_0 = -0.7764$ a.u. and the equilibrium internuclear separation $\langle R \rangle = 2.643$ a.u. obtained from the lowest eigenvalue of Eq. (45) and the R-expectation value of the corresponding wave function $\chi(R)$, nicely agree with the exact results of $E_0 = -0.7764$ and $\langle R \rangle = 2.645$ as displayed in Table 1. For larger internuclear distances, we observe small deviations from the Born–Oppenheimer curve. The Hartree approach, on the other hand, performs significantly worse. The equilibrium distance and ground-state energy are still reasonable (see Table 1) but, as displayed in Fig. 1 the effective nuclear potential starts to deviate strongly from the BO curve for distances larger than the equilibrium distance. The reason for this large deviation is, a explained in [39,42], related to the simple uncorrelated structure of the Hartree wavefunction. In this approximation the conditional probability distribution of the electrons for a given internuclear separation, which may be defined as

$$\rho_{\mathrm{cond}}(z,t|R) = \frac{|\Psi(R,z,t)|^2}{N(R,t)}, \tag{64}$$

is independent of the nuclear separation, i.e. in the Hartree approximation for the wavefunction we have $\rho_{\mathrm{cond}}(z,t|R) = |\varphi(z,t)|^2$. When the energy is optimized we find a conditional electron distribution that is reasonable for

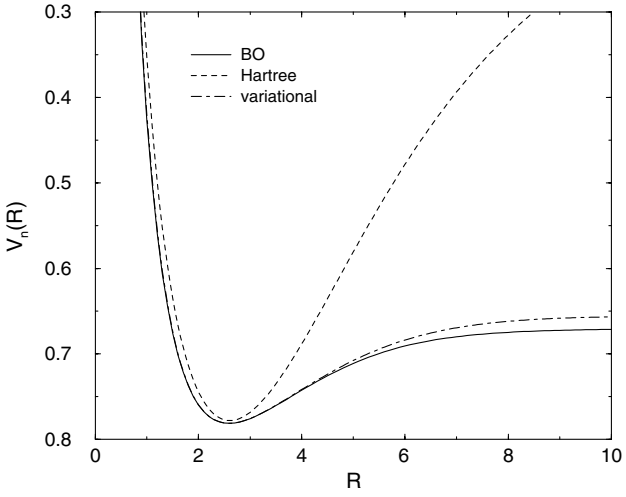

Fig. 1. Effective nuclear potential $V_n(R) = \langle \hat{H} \rangle_e(R)$ obtained for the model H_2^+ molecule from a self-consistent solution of the variational approach. For comparison, the nuclear potentials resulting from the BO and the Hartree approximations are added to the plot. All quantities are given in atomic units.

Table 1
Summary of results for the model H_2^+ molecule obtained from self-consistent solutions of the Hartree and the correlated variational scheme compared with results from exact and BO calculations

	Exact	BO	Hartree	Variational
$-E_0$	0.7764	0.7764	0.7748	0.7764
$\langle R \rangle$	2.645	2.642	2.629	2.643

All numbers in atomic units.

the equilibrium separation but very unrealistic at large internuclear distances. This is the cause of the unrealistic shape of the nuclear Hartree potential at large internuclear distances. One may expect that these deviations of the nuclear Hartree potential will lead to severe errors in the description of the dissociation dynamics using the time-dependent Hartree approach. We will see that this is indeed the case. The correlated variational scheme, on the other hand, promises a much more adequate treatment of the strong-field dynamics. Moreover, the small remaining deviations of the variational nuclear potential for large internuclear separations may not seriously harm, because the time-dependent nuclear potential will adjust to the changes of the nuclear density. In this sense our approach is very different from approaches of wavepacket propagation on fixed, i.e. time-independent, Born–Oppenheimer surfaces.

5.2. Time propagation

In the following, we solve the exact Schrödinger equation and our models for the model-H_2^+ molecule in a $\lambda = 228$ nm laser field corresponding to a photon energy of $\omega = 0.2$ a.u. This energy has been chosen to give substantial ionization as well as dissociation probabilities and therefore to give a strong interplay between electronic and nuclear dynamics. The radiation field is linearly ramped to its maximum strength over 10 optical cycles and subsequently held constant for an additional 15 laser cycles, corresponding to a total propagation time of about 19 fs. We have performed calculations employing four different peak intensities ranging from $I_0 = 2.5 \times 10^{13}$ to $I_0 = 2 \times 10^{14}$ W/cm^2.

The numerical parameters for the exact Schrödinger equation and the Hartree equations that are solved on a numerical grid in R and z are given in Table 2. For the correlated ansatz the numerical parameters are given in Table 3. For this system we use a grid in momentum space. Accordingly, electronic momenta up to $k \approx 7.9$ a.u. can be represented with a resolution of $\Delta_k \approx 0.04$ a.u. on the chosen grid. In configuration space, this corresponds to a lattice spacing of $\Delta_z = 0.4$ a.u. and a total extension of the grid of about 150 a.u., which allows for a proper description of the strong-field dynamics. Depending on the peak intensity, a temporal resolution of 10,000–30,000 integration steps per laser cycle is needed to obtain stable and converged results.

Before the laser field is turned on, the molecule is prepared in its ground state, which therefore serves as initial state of the time propagation. The initial ground state is determined by imaginary-time propagation employing the same numerical scheme as described for the full time-dependent problem. Therefore, spurious excited-state contaminations are avoided.

In Figs. 2–4, we summarize the results obtained for the time evolution of the mean internuclear distance

$$\langle R \rangle(t) = \frac{\int_{\text{grid}} \mathrm{d}R R N(R,t)}{\int_{\text{grid}} \mathrm{d}R N(R,t)}, \tag{65}$$

and the ionization probability and total dissociation probability

$$P_{\text{diss}}(t) = 1 - \int_{\text{box}_n} \mathrm{d}R N(R,t), \tag{66}$$

$$P_{\text{ion}}(t) = 1 - \int_{\text{box}_e} \mathrm{d}z \rho(z,t), \tag{67}$$

Table 2
Parameters used in the numerical solution of the exact and Hartree equations for the model H_2^+ molecule

N_R	Δ_R (a.u.)	$R_{\max}$ (a.u.)	N_z	Δ_z (a.u.)	$\lvert z_{\max}\rvert$ (a.u.)	N_τ
384	0.1	38.8	768	0.4	153.4	500

A nuclear finite-difference grid (characterized by the first three columns of the table displaying the number over grid points, the grid spacing and the maximum grid value), as well as an electronic finite difference grid (characterized by the next three columns of the table) is employed. The quantity N_τ in the last column denotes the number of time steps per optical cycle τ.

Table 3
Parameters used in the numerical solution of the time-dependent variational equations for the model H_2^+ molecule

N_R	Δ_R (a.u.)	$R_{\max}$ (a.u.)	N_k	Δ_k (a.u.)	$\lvert k_{\max}\rvert$ (a.u.)
256	0.1	26.0	384	0.04	7.9

The nuclear equation of motion is discretized on a finite-difference grid (characterized by the first three columns of the table), whereas the electronic equations of motion are represented in momentum space (characterized by the last three columns of the table) employing a uniform distribution of the k points.

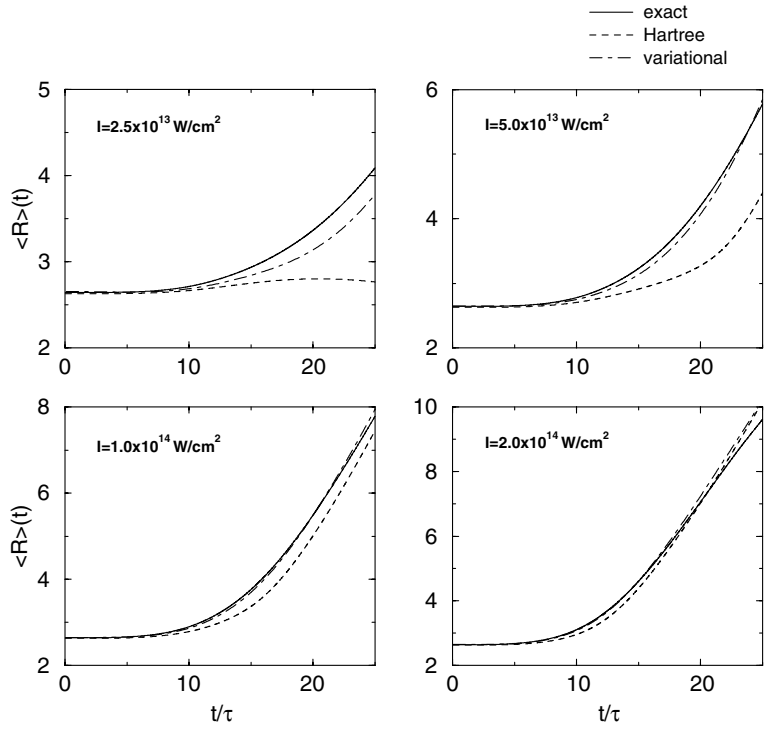

Fig. 2. Time evolution (in units of the optical cycle τ) of the mean internuclear distance $\langle R\rangle(t)$ obtained for the model H_2^+ molecule in a $\lambda = 228$ nm laser field with different intensities from the exact solution, the time-dependent mean-field (Hartree) approximation, and the time-dependent correlated approach.

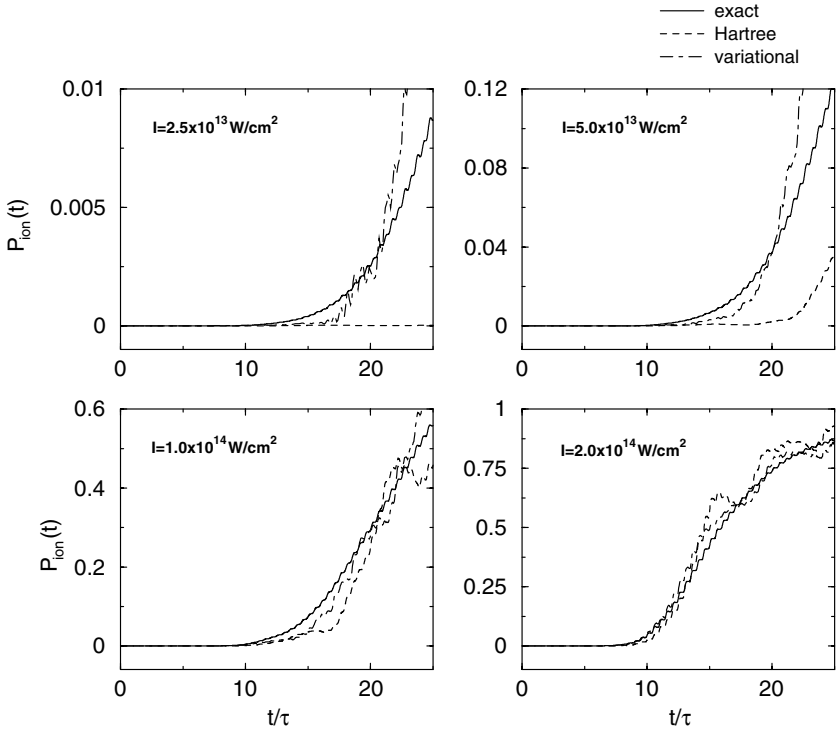

Fig. 3. Time evolution (in units of the optical cycle τ) of the ionization probability $P_{\mathrm{ion}}(t)$ obtained for the model H_2^+ molecule in a $\lambda = 228$ nm laser field with different intensities from the exact solution, the time-dependent mean-field (Hartree) approximation, and the time-dependent correlated approach.

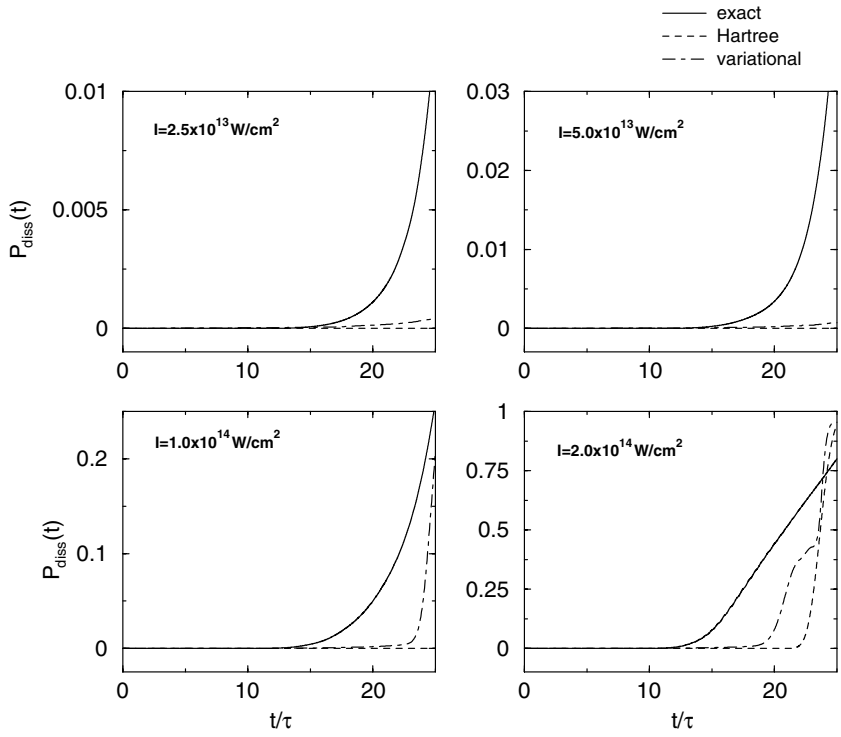

Fig. 4. Time evolution (in units of the optical cycle τ) of the total dissociation probability $P_{\mathrm{diss}}(t)$ obtained for the model H_2^+ molecule in a $\lambda = 228$ nm laser field with different intensities from the exact solution, the time-dependent mean-field (Hartree) approximation, and the time-dependent correlated approach.

respectively, where the nuclear and electronic densities are obtained from Eqs. (8) and (9) for the exact wavefunction. For the Hartree and the correlated approach they are evaluated using expressions (10)–(13). According to the above prescription, ionization and dissociation probabilities are evaluated by means of a geometrical concept. It rests on the assumption that the relevant bound states of the system under consideration are contained inside some suitably chosen finite volume of the numerical grid. The continuum part of the wavefunction, on the other hand, will cross the boundaries of this "analyzing volume" and – sooner or later – leave the total grid. As a result, the probability remaining inside the analyzing volume will decrease and the outgoing flux leaving the "electronic analyzing box" or "nuclear analyzing box" ($\mathrm{box}_{\mathrm{e/n}}$) is identified with ionized electrons or with a dissociated part of the molecule, respectively. Evidently, such a prescription is only approximate. It is valid if the physical observables calculated that way are insensitive to the chosen box sizes. Provided the volumes are reasonably large, this idea has been found useful in the context of strong-field phenomena [33,34,43] (for a general discussion of the method applied to multiple ionization see [44]). In the context of the present work, reasonable analyzing boxes are obtained by choosing $\mathrm{box}_{\mathrm{n}} = [0, \ldots, 9]$ a.u. and $\mathrm{box}_{\mathrm{e}} = [-10, \ldots, 10$ a.u.$]$.

To begin with, we consider the lowest intensity of $I_0 = 2.5 \times 10^{13}$ W/cm^2. Comparing the photon energy $\omega = 0.2$ a.u. to the dissociation energy $D_0 = 0.1066$ a.u. of the model molecule, we shall expect that the molecule easily disintegrates via the photodissociation channel ($H_2^+ \rightarrow H + H^+$), even for this comparatively low intensity. Indeed, in the upper-left plot of Fig. 2, the mean internuclear distance is seen to increase during the propagation, indicating that the molecule dissociates. Simultaneously, a low ionization probability is found in Fig. 3, which confirms the above conjecture that the molecule predominantly undergoes photodissociation. We note that, from the upper-left plot of Fig. 4, the total dissociation probability appears quite small, too. However, we just see the onset of the dissociation process in this plot. Since the nuclear motion is rather slow, most of the dissociative nuclear wavepackets have no yet reached the boundaries of the nuclear analyzing box at $R = 9$ a.u., which is also suggested by the small magnitude of $\langle R \rangle(t)$. A longer propagation confirms the above statement that photodissociation is the dominant process for the chosen intensity.

In the mean-field approach, on the other hand, the molecule does neither ionize nor dissociate but only starts to vibrate as seen from the oscillatory behavior of the mean internuclear distance in Fig. 5, thus showing the discussed shortcomings of the time-dependent mean-field approach.

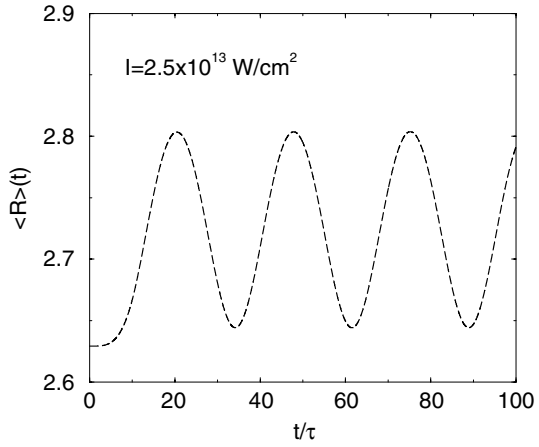

Fig. 5. Time evolution (in units of the optical cycle τ) of the mean internuclear distance $\langle R\rangle(t)$ obtained for the H_2^+ molecule in a $\lambda = 228$ nm laser field within the time-dependent Hartree approximation.

Turning to the results obtained from the correlated variational approach, we find a significant improvement upon the mean-field results. Although some deviations from the exact dynamics are still left, the time evolution of the mean internuclear separation resulting from the variational approach indicates a dissociation process, too, as shown in the upper-left plot of Fig. 2. Moreover, we also find reasonable agreement in the ionization behavior, as seen in the upper-left plot of Fig. 3. Thus, we can infer that the variational scheme deals with the photodissociation process in a much more realistic way than the mean-field approximation.

With increasing intensity, the differences between the exact and the variational solution in the time evolution of $\langle R\rangle(t)$ become smaller. Moreover, the variational scheme consistently improves upon the mean-field approximation and provides a reliable description for all intensities considered here. The same tendency is found for the ionization behavior, which is displayed in Fig. 3. At least on a qualitative level, the variational approach reproduces the exact behavior of $P_{\mathrm{ion}}(t)$. Furthermore, for the two highest intensities, both approximate schemes perform similarly and lead to satisfactory results. These observations thus suggest that the electronic and, in particular, the ionization dynamics is properly treated within the time-dependent variational approach.

Despite these improvements, Fig. 4 still reveals considerable deviations for the dissociation probability $P_{\mathrm{diss}}(t)$. In order to understand their origin, we consider the time evolution of the nuclear density $N(R,t)$, which is plotted in Fig. 6 for a peak intensity of 5×10^{13} W/cm^2. Evidently, the nuclear wavepackets obtained from the variational approach are

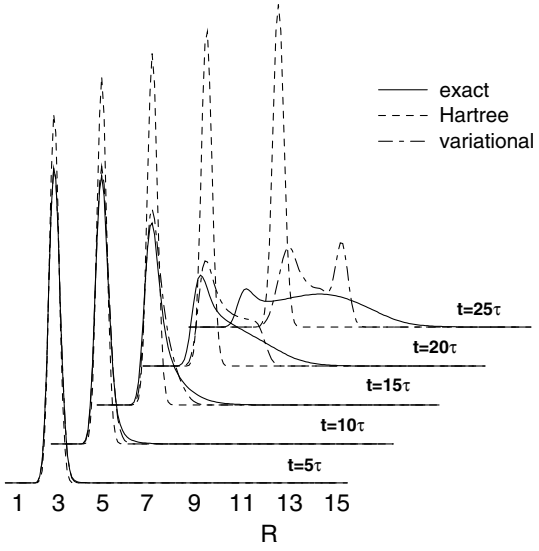

Fig. 6. Time evolution of the nuclear density $N(R,t)$ obtained for the model H_2^+ molecule in a $\lambda = 228$ nm, $I_0 = 5 \times 10^{13}$ W/cm^2 laser field from the exact solution, the time-dependent mean-field (Hartree) approximation, and the time-dependent correlated approach.

superior to the mean-field ones. Most notably, the variational scheme also predicts a splitting of the nuclear wave-packet, which is totally absent in the mean-field results. However, the densities are still too localized compared to the exact curves. In particular, the variational method cannot reproduce the long-reaching tails of the exact nuclear densities. Clearly, an integration of the various $N(R,t)$ shown in Fig. 6 over the nuclear "analyzing box" results in the differences depicted in Fig. 4. The deviations in the nuclear density can be traced back to deficiencies in the effective nuclear potential. Those, in turn, are caused by the fact that only one atomic orbital (per atom) is used to evaluate the nuclear potential in the entire range of internuclear distances. Since, by virtue of Eqs. (32) and (33), the atomic orbital is determined by an averaged nuclear configuration, it is always "optimized" for, loosely speaking, the most probable internuclear distance. Such a procedure will provide a reasonable description for densities which are rather narrow functions in space. For the time-dependent situation shown in Fig. 6, the approach provides a reasonable description of the mean dynamics, as seen from the upper-right plot of Fig. 2. Since, however, the atomic orbital is dominated (at least up to $t \approx 20\tau$) by the small-R regime, the large-R behavior of the nuclear potential is less well represented, leading to the too contracted nuclear densities found, e.g., in Fig. 6. Moreover, for strongly delocalized nuclear densities as, e.g., for $N(R, t = 25\tau)$ in Fig. 6, the use of one and the same atomic orbital for the entire R range appears as a too severe restriction and leads to the deviations observed in the results.

6. Outlook: larger molecules

Even for molecules as small as H_2, the full three-dimensional solution of the time-dependent Schrödinger equation in the presence of a strong laser field represents a borderline case for present-day computer technology. In view of this fact, there is a clear need for reliable, yet feasible ab initio techniques. The goal of the above-described work on the one-dimensional model of H_2^+ was to prepare the ground for treating larger molecules. Already the case of many-electron diatomics (in three spatial dimensions) represents a formidable challenge. We therefore discuss this important case in some detail below. At the end of this section, we proceed to polyatomic molecules.

Arbitrary many-electron diatomics exposed to laser fields of high (but still non-relativistic) intensities are described by the Hamiltonian

$$\hat{H}(t) = -\frac{1}{2M_1}\nabla^2_{\mathbf{R}_1} - \frac{1}{2M_2}\nabla^2_{\mathbf{R}_2} + \sum_{i=1}^{N} -\frac{1}{2}\nabla^2_{\mathbf{r}_i} + \hat{W}_{\mathrm{nn}} + \hat{W}_{\mathrm{ee}} + \hat{W}_{\mathrm{en}} + \hat{V}_{\mathrm{laser}}(t), \tag{68}$$

where $\mathbf{r}_i$ are the N electronic variables and $\mathbf{R}_1$ and $\mathbf{R}_2$ denote the positions of the two nuclei with masses M_1 and M_2 and charges Z_1 and Z_2. Both nuclear and electronic positions refer to an inertial ("laboratory") frame. The terms W_{nn}, W_{en} and W_{ee} describe the nuclear–nuclear, electron–nuclear and electron–electron interactions, and $\hat{V}_{\mathrm{laser}}(t)$ represents the interaction of the electrons and the nuclei with the external laser field in dipole approximation

$$\hat{V}_{\mathrm{laser}}(t) = \left(\sum_{i=1}^{N}\mathbf{r}_i - Z_1\mathbf{R}_1 - Z_2\mathbf{R}_2\right)\mathbf{E}(t). \tag{69}$$

$\mathbf{E}(t)$ is the electric field of the laser which is assumed here to be linearly polarized. A major complication, compared to the one-dimensional model discussed in the previous sections, is the fact that in three dimensions the molecule need not be oriented parallel to the polarization axis of the laser. In fact, the time evolution of the molecular orientation is an important observable to be investigated. To deal with this problem we first perform a suitable coordinate transformation: clearly, the total center-of-mass position $\mathbf{R}_{\mathrm{CM}} = (M_1\mathbf{R}_1 + M_2\mathbf{R}_2 + \sum_{i=1}^{N}\mathbf{r}_i)/(M_1 + M_2 + N)$ of the whole molecule and the internuclear vector $\mathbf{R} = \mathbf{R}_1 - \mathbf{R}_2$ represent a favourable choice. Furthermore, the electronic coordinates are transformed such that they refer to a frame attached to the nuclei. To this end we define an orthogonal matrix $\mathscr{D}$ which rotates the internuclear vector $\mathbf{R}$ into a position parallel to the z-axis of the laboratory frame, i.e. $\mathscr{D}\mathbf{R} = R\mathbf{e}_z$, where $R = |\mathbf{R}|$. This matrix can be parametrized by two angles θ and φ describing the orientation of $\mathbf{R}$ with respect to the laboratory z-axis. For the electronic coordinates we then introduce the new variables

$$\mathbf{r}'_i = \mathscr{D}(\mathbf{r}_i - \mathbf{R}_{\mathrm{CMN}}), \tag{70}$$

where $\mathbf{R}_{\mathrm{CMN}} = (M_1\mathbf{R}_1 + M_2\mathbf{R}_2)/(M_1 + M_2)$ is the center of mass of the nuclei. This means that the electronic coordinates are centered on the nuclear center of mass and rotated with the same transformation that takes the internuclear vector into a position parallel to the z-axis. Thus, the complete set of new coordinates is $(\mathbf{R}_{\mathrm{CM}}, R, \theta, \varphi, \mathbf{r}'_i)$. In terms of these coordinates, the transformed Hamiltonian has the following form:

$$\hat{H}(t) = \hat{H}_{\mathrm{CM}}(t) + \hat{H}_{\mathrm{mol}}(t), \tag{71}$$

where

$$\hat{H}_{\mathrm{CM}}(t) = -\frac{1}{2M_{\mathrm{tot}}}\nabla^2_{\mathbf{R}_{\mathrm{CM}}} - Q_{\mathrm{tot}}\mathbf{R}_{\mathrm{CM}}\mathbf{E}(t). \tag{72}$$

Here $M_{\mathrm{tot}} = M_1 + M_2 + N$ is the total mass and $Q_{\mathrm{tot}} = Z_1 + Z_2 - N$ the total charge of the molecule. The "internal" molecular Hamiltonian is given by

$$\begin{aligned}\hat{H}_{\mathrm{mol}}(t) = &-\frac{1}{2\mu_{\mathrm{n}}}\nabla^2_{\mathbf{R}} + W_{\mathrm{nn}}(\mathbf{R}) + \sum_{i=1}^{N}\left(-\frac{1}{2}\nabla^2_{\mathbf{r}'_i} + W_{\mathrm{en}}(\mathbf{r}'_i,\mathbf{R})\right) + \sum_{i>j}^{N} W_{\mathrm{ee}}(\mathbf{r}'_i - \mathbf{r}'_j) + \hat{T}_{\mathrm{MP}}(\mathbf{r}'_1,\mathbf{r}'_2,\ldots,\mathbf{r}'_N)\\ &+ \hat{T}_{\mathrm{C}}(\mathbf{r}'_1,\mathbf{r}'_2,\ldots,\mathbf{r}'_N,\mathbf{R}) - \mathscr{D}^{-1}\left(q_{\mathrm{n}}R\mathbf{e}_z - q_{\mathrm{e}}\sum_{i=1}^{N}\mathbf{r}'_i\right)\mathbf{E}(t),\end{aligned} \tag{73}$$

where $\mu_{\mathrm{n}} = M_1M_2/(M_1+M_2)$ is the nuclear reduced mass and

$$q_{\mathrm{n}} = (Z_1M_2 - Z_2M_1)/(M_1+M_2), \tag{74}$$

$$q_{\mathrm{e}} = (Z_1 + Z_2 + M_1 + M_2)/M_{\mathrm{tot}}. \tag{75}$$

The interaction potentials W_{nn}, W_{en} and W_{ee} are given by

$$W_{\mathrm{nn}}(\mathbf{R}) = \frac{Z_1Z_2}{R}, \tag{76}$$

$$W_{\mathrm{ee}}(\mathbf{r}'_i - \mathbf{r}'_j) = \frac{1}{|\mathbf{r}'_i - \mathbf{r}'_j|}, \tag{77}$$

$$W_{\mathrm{en}}(\mathbf{r}'_i,\mathbf{R}) = -\frac{Z_1}{|\mathbf{r}'_i - \frac{M_2}{M_1+M_2}R\mathbf{e}_z|} - \frac{Z_2}{|\mathbf{r}'_i + \frac{M_1}{M_1+M_2}R\mathbf{e}_z|}. \tag{78}$$

The mass-polarization term $\hat{T}_{\mathrm{MP}}$ has the explicit form

$$\hat{T}_{\mathrm{MP}} = -\frac{1}{2(M_1+M_2)}\sum_{i,j=1}^{N}\nabla_{\mathbf{r}'_i}\cdot\nabla_{\mathbf{r}'_j}. \tag{79}$$

The term $\hat{T}_{\mathrm{C}}$ represents the Coriolis forces which appear as a consequence of the fact that the electrons are now viewed from a non-inertial frame. It is given by [46]

$$\hat{T}_{\mathrm{C}} = -\frac{1}{2\mu_{\mathrm{n}}R^2}\left\{\frac{\partial}{\partial R}R^2\frac{\partial}{\partial R} + \frac{1}{\sin\theta}\left(\frac{\partial}{\partial\theta} - \mathrm{i}\hat{L}_{\mathrm{e},y}\right)\sin\theta\left(\frac{\partial}{\partial\theta} - \mathrm{i}\hat{L}_{\mathrm{e},y}\right) + \frac{1}{\sin^2\theta}\left(\frac{\partial}{\partial\varphi} + \mathrm{i}\hat{L}_{\mathrm{e},x}\sin\theta - \mathrm{i}\hat{L}_{\mathrm{e},z}\cos\theta\right)^2\right\} + \frac{1}{2\mu_{\mathrm{n}}}\nabla^2_{\mathbf{R}}, \tag{80}$$

where $\hat{L}_{\mathrm{e}}$ denotes the total electronic angular momentum operator.

Our next task is to find a variational form of the full wavefunction Ψ that leads to equations of motion with a sufficiently simple one-particle structure. In this way our method will stay computationally manageable, even for general diatomics. We choose the form

$$\Psi(\mathbf{r}'_1\cdots\mathbf{r}'_N,\mathbf{R},\mathbf{R}_{\mathrm{CM}},t) = \Psi_{\mathrm{CM}}(\mathbf{R}_{\mathrm{CM}},t)\chi(\mathbf{R},t)\Phi(\mathbf{r}'_1\cdots\mathbf{r}'_N,\mathbf{R},t). \tag{81}$$

Here Ψ_{CM} describes the center-of-mass motion, $\chi(\mathbf{R},t)$ represents an internal nuclear wavefunction and Φ is a Slater determinant of electronic molecular orbitals given by

$$\Phi(\mathbf{r}'_1\cdots\mathbf{r}'_N,\mathbf{R},t) = \frac{1}{\sqrt{N!}}|\phi_1(\mathbf{r}'_1,\mathbf{R},t)\cdots\phi_N(\mathbf{r}'_N,\mathbf{R},t)|. \tag{82}$$

Similar to the case of H_2^+ we will write each of the molecular orbitals as a sum over atomic-like orbitals attached to the two nuclei

$$\phi_i(\mathbf{r}',\mathbf{R},t) = \phi_{i,1}\left(\mathbf{r}' - \frac{M_2}{M_1+M_2}R\mathbf{e}_z,t\right) + \phi_{i,2}\left(\mathbf{r} + \frac{M_1}{M_1+M_2}R\mathbf{e}_z,t\right), \tag{83}$$

where $R = |\mathbf{R}|$. If we insert the Hamiltonian of Eq. (71) and the approximate form for the wavefunction of Eq. (81) in the variational equation (5) we obtain $2N+2$ equations of motion with effective one-particle Hamiltonians. These equations have the form

$$\mathrm{i}\partial_t \Psi_{\mathrm{CM}}(\mathbf{R}_{\mathrm{CM}},t) = \hat{H}_{\mathrm{CM}}(\mathbf{R}_{\mathrm{CM}},t)\Psi_{\mathrm{CM}}(\mathbf{R}_{\mathrm{CM}},t), \tag{84}$$

$$\mathrm{i}\partial_t \chi(\mathbf{R},t) = \hat{h}_{\mathrm{n}}(\mathbf{R},t)\chi(\mathbf{R},t), \tag{85}$$

$$\mathrm{i}\partial_t \phi_{i,j}(\mathbf{r}',t) = \hat{h}_{\mathrm{e},i,j}(\mathbf{r}',t)\phi_{i,j}(\mathbf{r}',t) + \mathscr{Q}_{i,j}(\mathbf{r}',t). \tag{86}$$

The detailed form of these equations will be presented elsewhere. For the case $N = 1$ in one dimension these equations reduce to the equations of motion for the model H_2^+ molecule that we obtained before. We should further note that the approximate wavefunction of Eq. (81) is invariant under the transformation

$$\chi \to \left(\prod_{i=1}^{N} c_i(t)\right)\chi, \tag{87}$$

$$\phi_i \to \frac{1}{c_i(t)}\phi_i, \tag{88}$$

where $c_i(t)$ are arbitrary complex functions of time. As a consequence we need N additional complex constraints to provide a unique solution to the equations of motion. These can be chosen to one's convenience. One choice could be to require that

$$\langle \phi_i | \partial_t \phi_i \rangle = 0 \tag{89}$$

which would lead to Lagrange multipliers $\Lambda_i(t)$ in Eq. (86) analogous to the $\Lambda(t)$ of Eq. (27). We further note that we did note introduce a time-dependent factor for the center-of-mass wave function Ψ_{CM}. This is because Ψ_{CM} satisfies the equation of motion, Eq. (84), with the hermitian Hamiltonian of Eq. (72) and therefore its norm is conserved and its phase is completely determined by its initial state.

We have now completely defined the equations of motion for a general diatomic molecule. Let us now discuss the applicability and validity of these equations. They are of similar structure as those of the H_2^+ molecule and can hence be solved by the same numerical techniques. A notable difference to the one-dimensional model of H_2^+ is the presence of the electron–electron interactions W_{ee}, T_{MP} and T_{C}. Within the approximate form of the wavefunction given in Eq. (81), all these interactions are treated in a Hartree–Fock manner. We emphasize that the mass-polarization and Coriolis terms do not present a serious obstacle in this context. The expectation value with respect to the above determinantal wavefunction is straightforwardly calculated, yielding

$$\langle T_{\mathrm{MP}} \rangle = -\frac{1}{2(M_1+M_2)}\left\{ \sum_{jk} \int \mathrm{d}\mathbf{r}\, \mathrm{d}\mathbf{r}' \phi_j^*(\mathbf{r}) \nabla_{\mathbf{r}} \phi_j(\mathbf{r}) \phi_k^*(\mathbf{r}') \nabla_{\mathbf{r}'} \phi_k(\mathbf{r}') - \sum_{jk} \int \mathrm{d}\mathbf{r}\, \mathrm{d}\mathbf{r}' \phi_j^*(\mathbf{r}) \nabla_{\mathbf{r}} \phi_k(\mathbf{r}) \phi_k^*(\mathbf{r}') \nabla_{\mathbf{r}'} \phi_j(\mathbf{r}') \right\} \tag{90}$$

and

$$\begin{aligned} \langle T_{\mathrm{C}} \rangle = \int \mathrm{d}\mathbf{R} \chi^*(\mathbf{R}) \frac{1}{2\mu_{\mathrm{n}} R^2} \Bigg\{ & \mathrm{i}\langle \hat{L}_{\mathrm{e},y} \rangle_{\mathrm{e}} \left(\cot\theta + 2\frac{\partial}{\partial\theta} \right) - 2\langle \hat{L}_{\mathrm{e},x} \hat{L}_{\mathrm{e},z} \rangle_{\mathrm{e}} \cot\theta + \langle \hat{L}_{\mathrm{e},x}^2 + \hat{L}_{\mathrm{e},y}^2 \rangle_{\mathrm{e}} + \langle \hat{L}_{\mathrm{e},z}^2 \rangle_{\mathrm{e}} \cot^2\theta \\ & + 2\mathrm{i}\left(\langle \hat{L}_{\mathrm{e},z} \rangle_{\mathrm{e}} \cot\theta - \langle \hat{L}_{\mathrm{e},y} \rangle_{\mathrm{e}} \right) \frac{1}{\sin\theta} \frac{\partial}{\partial\varphi} \Bigg\} \chi(\mathbf{R}), \end{aligned} \tag{91}$$

where the subscript "e" indicates that the integration is over electronic coordinates only. Whether this mean-field treatment of the electronic interactions is sufficiently accurate depends on the laser intensity and frequency regime, as well as on the physical property one is interested in. Since little is known about electron correlation in strong laser fields it would therefore be desirable to test the variational wavefunction (81) first for a model H_2 that can be solved exactly [35]. If necessary, it is possible to extend the ansatz of Eq. (81) to explicitly include electronic correlations without destroying the effective one-particle structure of the equations of motion. One could, for instance, variationally optimize a wavefunction of the form

$$\Psi(\mathbf{r}_1' \cdots \mathbf{r}_N', \mathbf{R}, \mathbf{R}_{\mathrm{CM}}, t) = \Psi_{\mathrm{CM}}(\mathbf{R}_{\mathrm{CM}}, t)\chi(\mathbf{R},t)\Phi(\mathbf{r}_1' \cdots \mathbf{r}_N', \mathbf{R}, t) \prod_{i>j}^{N} f(\mathbf{r}_i' - \mathbf{r}_j', t), \tag{92}$$

where Φ is defined as before and where f represents an electronic correlation factor. When we optimize this wavefunction with the stationary action principle we then obtain an additional effective equation for the correlation factor f. However, for molecules with a large number of electrons the construction of the effective Hamiltonians will now require a large computational effort due to the repeated integrations over the electronic coordinates. Nevertheless, with this method few-electron diatomics are still within reach of current computational technology.

We finally consider polyatomic molecules having K nuclei with charges $Z_1, \ldots, Z_K$ and masses $M_1, \ldots, M_K$. As before, N denotes the number of electrons. The first question to be addressed is the proper choice of coordinates in

terms of which the variational wavefunction is being formulated. As in the diatomic case, we represent the electronic degrees of freedom in a body-fixed coordinate frame attached to the nuclear center of mass

$$\mathbf{r}'_i = \mathscr{D}(\alpha,\beta,\gamma)(\mathbf{r}_i - \mathbf{R}_{\mathrm{CMN}}), \tag{93}$$

where $\mathbf{R}_{\mathrm{CMN}} = (\sum_{\nu=1}^{K} M_\nu \mathbf{R}_\nu)/(\sum_{\nu=1}^{K} M_\nu)$. $\mathscr{D}$ is an orthogonal matrix which rotates the principal axes of the nuclear inertia tensor into the axes of the laboratory frame and α,β,γ are the Euler angles associated with this three-dimensional rotation. α,β,γ are functions of the nuclear coordinates $\mathbf{R}_1,\ldots,\mathbf{R}_K$. Other choices for the body-fixed coordinate frame have been employed in the literature [46]. Apart from this definition of the electronic coordinates, we use the total center of mass $\mathbf{R}_{\mathrm{CM}}$ of all electrons and nuclei, and a set of suitably chosen collective coordinates $\underline{\mathbf{Q}} = (Q_1,\ldots,Q_{3K-3})$ describing the nuclear degrees of freedom. The Euler angles α,β,γ and hence the rotational matrix $\mathscr{D}$ then become functions of $\underline{\mathbf{Q}}$. In terms of this set of new coordinates, the interaction of the laser with all electrons and nuclei can be written as

$$\hat{V}_{\mathrm{laser}}(t) = -Q_{\mathrm{tot}}\mathbf{R}_{\mathrm{CM}}\mathbf{E}(t) + \mathscr{D}^{-1}(\underline{\mathbf{Q}})\left(-\sum_{\alpha=1}^{K} Z_\alpha \mathbf{R}'_\alpha(\underline{\mathbf{Q}}) + q_{\mathrm{e}}\left(\sum_{i=1}^{N}\mathbf{r}'_i\right)\right)\mathbf{E}(t), \tag{94}$$

where

$$\mathbf{R}'_\alpha(\underline{\mathbf{Q}}) = \mathscr{D}(\underline{\mathbf{Q}})(\mathbf{R}_\alpha(\underline{\mathbf{Q}}) - \mathbf{R}_{\mathrm{CMN}}(\underline{\mathbf{Q}})). \tag{95}$$

Here $Q_{\mathrm{tot}} = (\sum_{\alpha=1}^{K} Z_\alpha - N)$ is the total charge of the molecule and $q_{\mathrm{e}} = (Q_{\mathrm{tot}}/M_{\mathrm{tot}} + 1)$ with $M_{\mathrm{tot}} = (\sum_{\alpha=1}^{K} M_\alpha + N)$ being the total mass. The first term on the right-hand side of Eq. (94) and the center-of-mass kinetic energy operator are the only terms in the total Hamiltonian containing $\mathbf{R}_{\mathrm{CM}}$, which shows that the motion of the total center of mass can again be separated off from the wavefunction. The electron–nuclear interaction, in terms of the new coordinates, is given by

$$W_{\mathrm{en}}(\mathbf{r}'_i,\underline{\mathbf{Q}}) = -\sum_{\alpha=1}^{K}\frac{Z_\alpha}{|\mathbf{r}'_i - \mathbf{R}'_\alpha(\underline{\mathbf{Q}})|}. \tag{96}$$

This suggests the following ansatz for the total wave function:

$$\Psi(\mathbf{r}'_1\cdots\mathbf{r}'_N,\underline{\mathbf{Q}},\mathbf{R}_{\mathrm{CM}},t) = \Psi_{\mathrm{CM}}(\mathbf{R}_{\mathrm{CM}},t)X(\underline{\mathbf{Q}},t)\Phi(\mathbf{r}'_1\cdots\mathbf{r}'_N,\underline{\mathbf{Q}},t). \tag{97}$$

As in the diatomic case, Φ is a determinant (82) of electronic single-particle orbitals ϕ_i. The latter are expressed as superpositions of atomic-like orbitals, each of which is centered on one nucleus

$$\phi_i(\mathbf{r}',\underline{\mathbf{Q}},t) = \sum_{\alpha=1}^{K}\phi_{i,\alpha}(\mathbf{r}' - \mathbf{R}'_\alpha(\underline{\mathbf{Q}}),t). \tag{98}$$

The nuclear wave function $X(\underline{\mathbf{Q}},t)$ is approximated as a Hartree product

$$X(\underline{\mathbf{Q}},t) = \chi_1(Q_1,t)\chi_2(Q_2,t)\cdots\chi_{3K-3}(Q_{3K-3},t) \tag{99}$$

or, better, as a finite linear combination of Hartree products. Such linear combinations are routinely employed in the multi-configuration time-dependent Hartree (MCTDH) method [47–49]. However, in standard MCTDH, the nuclei are propagated on *given* potential energy surfaces, which have to be determined in a separate calculation. The key feature of our formulation is that the forces on the nuclei (i.e. the effective potentials appearing in the nuclear Schrödinger equation) are calculated "on the fly". The accuracy of the nuclear wave function (99) crucially depends on the choice of the collective coordinates $\underline{\mathbf{Q}}$. Usually the proper choice requires some prior knowledge of the physical processes to be expected. For small-amplitude vibrations, standard normal coordinates should be an adequate choice, while for fragmentation, Jacobi coordinates may be preferred. An interesting alternative, not requiring any prior knowledge of the nuclear dynamics, may result from coordinates $\underline{\mathbf{Q}}$ which, themselves, are determined variationally. This idea was recently explored in time-independent situations [50].

7. Conclusions

The time-dependent variational scheme presented in this contribution provides a novel approach to the description of molecular strong-field phenomena. By construction, it allows for a treatment of non-perturbative as well as non-adiabatic processes and it properly accounts for the quantum mechanical nature of electronic and nuclear degrees of freedom. Employing the explicitly correlated ansatz (7) for the full time-dependent wavefunction, the variational

approach enables us to handle electron–nuclear correlation effects in the presence of strong laser pulses. It provides a – at least qualitatively – correct description of photodissociation processes. Similarly, the main aspects of strong-field electronic dynamics, including the strong R-dependence of the ionization rates or the CREI mechanism followed by dissociative Coulomb explosion, are reproduced within the variational scheme as well. Despite all these features, the variational scheme still leads to – sometimes substantial – deviations from the exact results. They are traced back to the fact that one and the same atomic orbital is used to describe the entire range of nuclear configurations – which appears reasonable for rather localized nuclear densities. However, for delocalized nuclear density distributions, this approach seems to impose a too severe restriction. While, in this communication, we restricted ourselves mainly to the H_2^+ molecule, the generalization to larger molecules, as indicated in the last section, is particularly promising due to the simple orbital structure of the method. Work along these lines is in progress.

Acknowledgements

This work was supported in part by the Deutsche Forschungsgemeinschaft, by the *EX!TiNG* Research and Training Network of the European Union and by the *NANOQUANTA* Network of Excellence. E.K.U.G. wishes to thank Ali Alavi, Garnet Chan and Michiel Sprik for inspiring discussions and the warm hospitality at the Cambridge University Computational Chemistry Centre where part of this work was done. A Schlumberger fellowship and a fellowship as visiting fellow at Trinity College, Cambridge are gratefully acknowledged.

References

[1] M. Perry, G. Mourou, Science 264 (1994) 917.
[2] G. Mourou, C. Barty, M. Perry, Phys. Today 51 (1998) 22.
[3] M. Rosker, M. Dantus, A. Zewail, Science 241 (1988) 1200.
[4] A. Zewail, Femtochemistry, vols. I and II, World Scientific, Singapore, 1994.
[5] J. Manz, in: V. Sundström (Ed.), Femtochemistry and Femtobiology: Ultrafast Reaction Dynamics at Atomic-Scale Resolution, Nobel Symposium, vol. 101, Imperial College Press, London, 1997, p. 80.
[6] A. Assion, T. Baumert, M. Bergt, T. Brixner, B. Kiefer, V. Seyfried, M. Strehle, G. Gerber, Science 282 (1998) 919.
[7] H. Rabitz, R. de Vivie-Riedle, M. Motzkus, K. Kompa, Science 288 (2000) 824.
[8] H. Niikura, P.B. Corkum, D.M. Villeneuve, Phys. Rev. Lett. 90 (2003) 203601.
[9] M. Gavrila (Ed.), Atoms in Intense Laser Fields, Academic Press, Boston, 1992.
[10] A. Bandrauk, S. Wallace (Eds.), Coherence Phenomena in Atoms and Molecules in Laser Fields, NATO ASI Series, Plenum Press, New York, 1992.
[11] B. Piraux, A. L'Huillier, K. Rzazewski (Eds.), Super-Intense Laser-Atom Physics, NATO ASI Series, Plenum Press, New York, 1993.
[12] H. Muller, M. Fedorov (Eds.), Super-Intense Laser-Atom Physics IV, NATO ASI Series, Kluwer Academic Publishers, Dordrecht, 1996.
[13] P. Lambropoulos, H. Walther (Eds.), Multiphoton Process 1996, IOP Publishing, Bristol, 1997.
[14] M. Protopapas, C. Keitel, P.L. Knight, Rep. Prog. Phys. 60 (1997) 389.
[15] A. Bandrauk (Ed.), Molecules in Laser Fields, Marcel Dekker, New York, 1994.
[16] S. Chelkowski, T. Zuo, A. Bandrauk, Phys. Rev. A 46 (1992) R5342.
[17] D. Dundas, J.F. McCann, J.S. Parker, K.T. Taylor, J. Phys. B 33 (2000) 3261.
[18] D. Dundas, Phys. Rev. A 65 (2000) 023408.
[19] D. Dundas, K.J. Meharg, J.F. McCann, K.T. Taylor, Eur. Phys. J. D 26 (2003) 51.
[20] S. Chelkowski, T. Zuo, O. Atabek, A.D. Bandrauk, Phys. Rev. A 52 (1995) 2977.
[21] F. Seyl, Ph.D. Thesis, Max-Planck-Institut für Strömungsforschung, Göttingen, 1996.
[22] S. Chelkowski, A. Conjusteau, T. Zuo, A.D. Bandrauk, Phys. Rev. A 54 (1996) 3235.
[23] I. Kawata, H. Kono, Y. Fujimura, Chem. Phys. Lett. 289 (1998) 546.
[24] I. Kawata, H. Kono, Y. Fujimura, J. Chem. Phys. 110 (1999) 11152.
[25] K.C. Kulander, F.H. Mies, K.J. Schafer, Phys. Rev. A 53 (1996) 2562.
[26] S. Chelkowski, C. Foisy, A.D. Bandrauk, Phys. Rev. A 57 (1998) 1176.
[27] A.D. Bandrauk, S. Chelkowski, J. Mol. Struct. 591 (2002) 199.
[28] J. Javanainen, J.H. Eberly, Q. Su, Phys. Rev. A 38 (1988) 3430.
[29] D.G. Lappas, A. Sanpera, J.B. Watson, K. Burnett, P.L. Knight, R. Grobe, J.H. Eberly, J. Phys. B 29 (1996) L619.
[30] D. Bauer, Phys. Rev. A 56 (1997) 3028.
[31] D.G. Lappas, R. van Leeuwen, J. Phys. B 31 (1998) L249.
[32] M. Lein, E.K.U. Gross, V. Engel, Phys. Rev. Lett. 22 (2000) 4707.
[33] N.E. Dahlen, R. van Leeuwen, Phys. Rev. A 64 (2001) 023405.
[34] N.E. Dahlen, Int. J. Mod. Phys. B 16 (2002) 415.
[35] M. Lein, T. Kreibich, E.K.U. Gross, V. Engel, Phys. Rev. A 65 (2002) 033403.
[36] T. Kreibich, M. Lein, V. Engel, E.K.U. Gross, Phys. Rev. Lett. 87 (2001) 103901.
[37] P.-O. Löwdin, P.K. Mukherjee, Chem. Phys. Lett. 14 (1972) 1.

[38] P. Kramer, M. Saraceno, Geometry of the Time-Dependent Variational Principle in Quantum Mechanics, Lecture Notes in Physics, vol. 140, Springer, Berlin, 1981.
[39] T. Kreibich, Multicomponent density-functional theory for molecules in strong laser fields, Ph.D. Thesis, Universität Würzburg, Shaker-Verlag, 2000.
[40] T. Zuo, A.D. Bandrauk, Phys. Rev. A 52 (1995) R2511.
[41] T. Seideman, M.Y. Ivanov, P.B. Corkum, Phys. Rev. Lett. 75 (1995) 2819.
[42] T. Kreibich, E.K.U. Gross, Phys. Rev. Lett. 86 (2001) 2984.
[43] K.C. Kulander, Phys. Rev. A 35 (1987) 445.
[44] C.A. Ullrich, J. Mol. Struct. 501–502 (2000) 315.
[45] W. Press, S. Teukolsky, W. Vetterling, B. Flannery, Numerical Recipes in Fortran 77, Cambridge University Press, Cambridge, 1992.
[46] P.R. Bunker, P. Jensen, Molecular Symmetry and Spectroscopy, NRC Research Press, Ottawa, 1998.
[47] H.-D. Meyer, U. Manthe, L.S. Cederbaum, Chem. Phys. Lett. 165 (1990) 73.
[48] U. Manthe, H.-D. Meyer, L.S. Cederbaum, J. Chem. Phys. 97 (1992) 3199.
[49] M. Nest, H.-D. Meyer, J. Chem. Phys. 117 (2002) 10499.
[50] N.I. Gidopoulos, J. Kohanoff, in preparation.